Dyes and Pigments 94 (2012) 481–489

Contents lists available at SciVerse ScienceDirect

Dyes and Pigments

journal homepage: www.elsevier.com/locate/dyepig

Performance of dye-sensitized solar cells based on novel sensitizers bearing asymmetric double D–π–A chains with arylamines as donors

Yanping Hong [a,c], Jin-Yun Liao [b], Jianlong Fu [a], Dai-Bin Kuang [b,**], Herbert Meier [d], Cheng-Yong Su [b], Derong Cao [a,*]

[a] School of Chemistry and Chemical Engineering, State Key Laboratory of Luminescent Materials and Devices, South China University of Technology, Guangzhou 510641, China
[b] MOE Key Laboratory of Bioinorganic and Synthetic Chemistry, KLGHEI of Environment and Energy Chemistry, School of Chemistry and Chemical Engineering, Sun Yat-sen University, Guangzhou 510275, China
[c] College of Food Science and Engineering, Laboratory of Plant Resource Exploitation and Utilization, Jiangxi Agricultural University, Nanchang 330045, China
[d] Institute of Organic Chemistry, University of Mainz, Mainz 55099, Germany

ARTICLE INFO

Article history:
Received 10 December 2011
Received in revised form
15 February 2012
Accepted 17 February 2012
Available online 25 February 2012

Keywords:
Dye-sensitized solar cell
Organic sensitizer
Organic dye
Donor-π-acceptor
Photovoltaic

ABSTRACT

Three novel, metal-free organic sensitizers bearing two asymmetric double donor-π-acceptor (D-π-A) chains (**DC1**-**3**), each, and a reference dye containing single D-π-A chain (**SC**) with cyanoacrylic acid as electron acceptor are synthesized. Their photophysical, electrochemical properties and the performances of the corresponding dye-sensitized solar cells (DSSCs) are further investigated. The dyes, **DC1**, **DC2** and **DC3** contain one chain with diphenylamine and another chain with carbazole or phenothiazine as electron donor, while diphenylamine is only employed as electron donor in **SC**. Compared to the inferior solar energy to electricity conversion efficiency (η) of 2.82%, 4.66% and 3.80%, respectively, for the DSSCs based on **DC1**, **DC2** and **SC**, the **DC3** sensitized cell gives η of 5.19% under standard global AM 1.5 solar condition (100 mW cm^{-2}) due to its broader and more intensive absorption in the UV–visible region.

1. Introduction

Dye-sensitized solar cells (DSSCs), as a promising photovoltaic device due to their relatively high efficiency and low-cost fabrication [1], have been received intense attention since the pioneering report in 1991 by Grätzel and coworkers [2]. As a critical component in DSSCs, the sensitizers play a vital role in providing electron injection into conduction band of TiO_2 upon light irradiation. Nowadays, the photoelectric conversion efficiencies of DSSCs sensitized by Zn-complex dyes have achieved maximal η over than 12% [3]. However, the limitations concerning these complexes such as rare sources, heavy-metal toxicity and environmental issues would limit their application. In recent years, metal-free organic dyes have been extensively developed as an alternative to noble metal-complexes due to their high molar extinction coefficients, ease of structure tailoring as well as low-cost synthesis process and compliance with environmental issues [4]. To date, hundreds of organic dyes have been explored to act as sensitizers for DSSCs and have obtained impressive efficiencies [4–17].

Organic dyes possessing a rod-like configuration with the electron-donating and electron-accepting groups bridged by a π-conjugated unit (D–π–A) are considered as one of the most promising classes of organic sensitizers. It is found that the photoinduced intramolecular electron transfer takes place in these dyes easily and the photophysical properties of the dyes can be easily tuned by varying donor, spacer, and acceptor moieties [18–20]. The results revealed that the DSSCs based on these D–π–A dyes showed better performances [8,21].

Recently, we reported a novel dye that contained double symmetric D–π–A chains (**DB**), and obtained an increased conversion efficiency of DSSCs compared to the corresponding single D–π–A dye since one molecule of **DB** contains two light harvesting units [14]. When asymmetric double D–π–A chains with diphenylamine and phenoxazine as donors were introduced into one dye molecule, the dye showed broad absorption range and better performance of its sensitized solar cells [15]. In order to get

* Corresponding author. Tel./fax: +86 20 87110245.
** Corresponding author. Tel.: +86 20 84113015.
E-mail addresses: kuangdb@mail.sysu.edu.cn (D.-B. Kuang), drcao@scut.edu.cn (D. Cao).

0143-7208/$ – see front matter © 2012 Elsevier Ltd. All rights reserved.
doi:10.1016/j.dyepig.2012.02.011

more insight into the impact on the performance of the solar cells under the conditions of introducing different donors or extending conjugated system into the sensitizers which bear asymmetric double D–π–A chains, here we designed a series of organic sensitizers with different arylamines as donors, such as diphenylamine, carbazole and phenothiazine (**DC1-3**). Moreover, a sensitizer with a single D–π–A chain was synthesized as reference (**SC**). As shown in Scheme 1, **DC1**, **DC2** and **DC3** were designed with the following characteristics: (i) the asymmetric D–π–A chains linked by non-conjugated n-hexane chain resulting two separate light harvesting systems would enhance the absorption intensity and broaden the absorption range due to the absorption overlap and complement of both the donors and π-spaces; at the same time, the linker of alkyl chain might be expected to depress aggregation of the dye on the TiO_2 surface [10,22], to increase the electron lifetime since the better surface protection, which would enhance the overall performance of the DSSCs [23]. (ii) in the D–π–A chains, different electron-donating capability donors of carbazole and phenothiazine were adopted to tune the HOMO and LUMO energy levels of the dyes to change the absorption range and intensity, which would affect the conversion efficiencies of the DSSCs.

2. Experimental section

2.1. Instrumentation and materials

^{1}H NMR and ^{13}C NMR spectra were recorded on a Bruker 400 MHz spectrometer in $CDCl_3$ or DMSO-d_6 with tetramethylsilane as inner reference. MS data were recorded on an Esquire HCT PLUS mass spectrometer. Elementary analyses were performed using a Vario EL*III* Analyzer. The melting point was taken on Tektronix X4 microscopic melting point apparatus and uncorrected. The absorption and emission spectra of the dyes in CH_2Cl_2/MeOH solution (2×10^{-5} M) were measured at room temperature by Shimadzu UV-2450 UV–Vis spectrophotometer and Fluorolog III photoluminescence spectrometer, respectively. Electrochemical redox potentials were obtained by cyclic voltammetry (CV) using a three-electrode cell and an electrochemistry workstation (e-corder (ED 401) potentiostat). The dyes sensitized TiO_2 films used as the working electrodes. The Ag/AgCl in saturated KCl solution and Pt wire were utilized as reference and counter electrodes with a scan rate of 50 mV/s. Tetrabutylammonium hexafluorophosphate ($TBAPF_6$) 0.1 M was used as

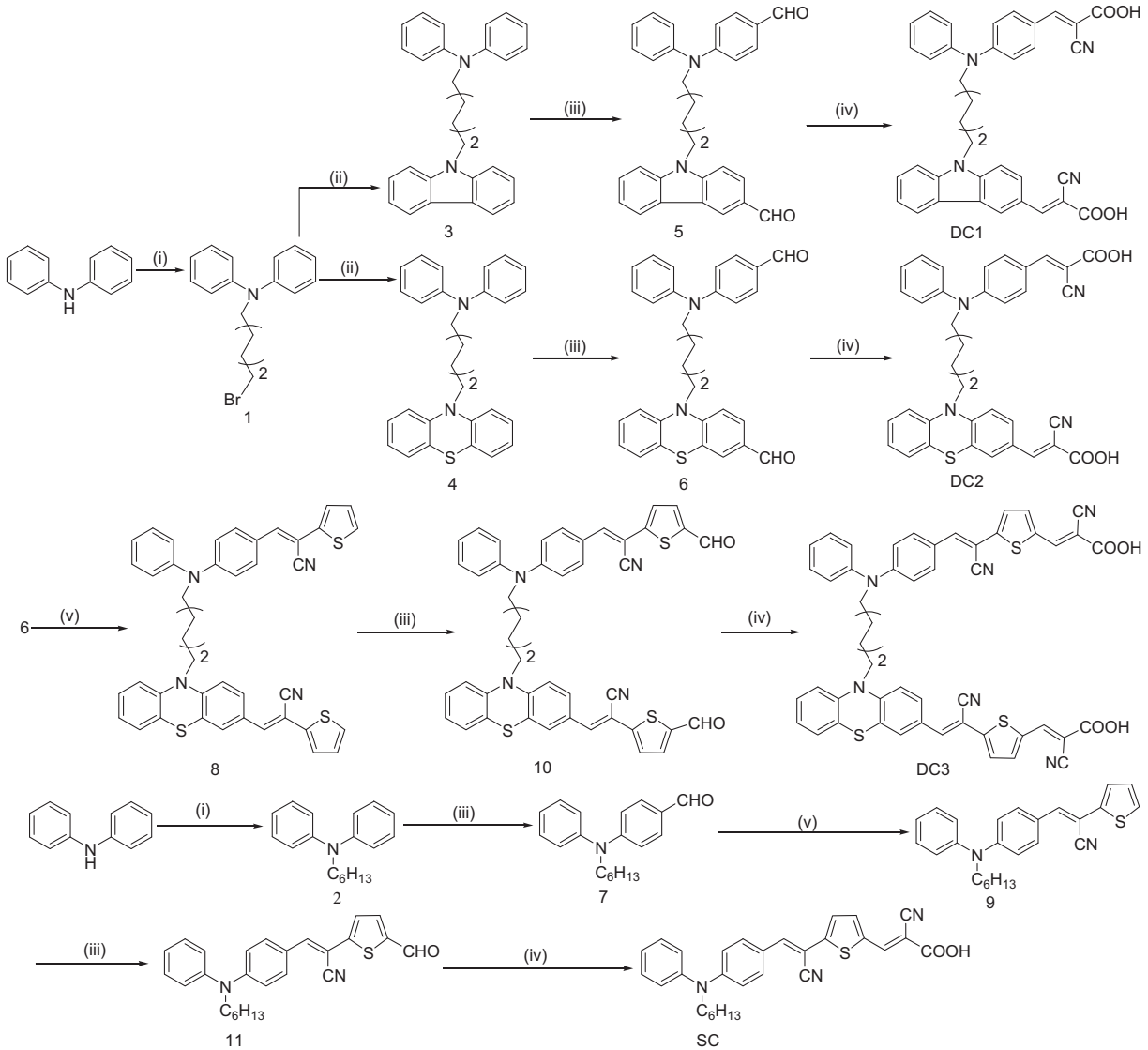

Scheme 1. Synthesis of the dyes **DC1**, **DC2**, **DC3** and **SC**. (i) 1,6-Dibromohexane or 1-bromohexane, NaH, $MeO(CH_2)_2OMe$, 85 °C, Ar, 2 h. (ii) Carbazole or phenothiazine, DMSO, KOH, N_2, rt, 3 h. (iii) $POCl_3$, DMF, ClC_2H_4Cl, 90 °C, N_2, 4 h. (iv) Cyanoacetic acid, $CHCl_3$, piperidine, reflux, 3 h. (v) 2-Thiopheneacetonitrile, t-BuOK, THF, reflux, 2 h.

supporting electrolyte in CH_3CN. The measurements were calibrated using ferrocene as standard. The redox potential of ferrocene internal reference is taken as 0.63 V versus normal hydrogen electrode (NHE). The current–voltage measurements were carried out by adopting a Keithley 2400 source meter under simulated AM 1.5 G illumination (100 mW cm^{-2}) provided by solar simulator (91192, Oriel). A 1 kW Xenon arc lamp (6271, Oriel) was served as a light source. The incident light intensity-was calibrated with a NREL standard Si solar cell. The IPCE spectra were measured as a function of wavelength from 350 to 800 nm on the basis of a Spectral Products DK240 monochromator. The electrochemical impedance spectroscopy (EIS) measurements were held on the Zahner Zennium electrochemical workstation in dark condition, with an applied bias of −0.7 V. A 10 mV AC sinusoidal signal was employed over the constant bias with the frequency ranging between 1 MHz and 10 mHz. Intensity-modulated photovoltage spectroscopy (IMVS) measurements were carried out on an electrochemical workstation (Zahner, Zennium) with a frequency response analyzer under a modulated green light emitting diodes (457 nm) driven by a source supply (Zahner, PP211), which provided both dc and ac components of the illumination. The modulated light intensity was 10% or less than the base light intensity. The frequency range was set from 100 kHz to 0.1 Hz.

2.2. Syntheses

(6-Bromo-hexyl)-diphenyl-amine (1). A solution of diphenylamine (6.76 g, 40 mmol), NaH (2.40 g, 60 mmol) in $MeO(CH_2)_2OMe$ (40 mL) was stirred at room temperature for 0.5 h under argon. Then, 1,6-dibromohexane (11.7 g, 48 mmol) was poured into the mixture and heated at 85 °C for 2 h. After cooling, the reaction mixture was filtered and the solvent was evaporated. The residue was purified by chromatography on a silica gel (petroleum) to give **1** (5.52 g, 41.7%) as a colorless liquid. ^{1}H NMR ($CDCl_3$, 400 MHz, ppm): δ 1.32–1.39 (m, 2H), 1.40–1.48 (m, 2H), 1.63–1.71 (m, 2H), 1.79–1.86 (m, 2H), 3.37 (t, J = 6.4 Hz, 2H), 3.68 (t, J = 7.6 Hz, 2H), 6.95 (m, 6H), 7.25 (m, 4H). ^{13}C NMR ($CDCl_3$, 100 MHz, ppm): δ 26.2, 27.3, 27.9, 32.6, 33.7, 52.1, 120.8, 121.1, 129.2, 148.0. ESI MS: m/z 331.1. Found: 330.3 $[M-H]^+$. Anal. Calcd. for $C_{18}H_{22}BrN$: C, 65.06; H, 6.67; N, 4.22. Found: C, 65.12; H, 6.69; N, 4.21.

Hexyl-diphenyl-amine (2). It was prepared as a colorless liquid in 74.2% yield from diphenylamine and 1-bromohexane by the same procedure established for **1**. ^{1}H NMR ($CDCl_3$, 400 MHz, ppm): δ 0.87 (t, J = 6.4 Hz, 3H), 1.28–1.36 (m, 6H), 1.61–1.69 (m, 2H), 3.67 (t, J = 7.6 Hz, 2H), 6.90–6.94 (m, 2H), 6.96–6.98 (m, 4H), 7.21–7.26 (m, 4H). ^{13}C NMR ($CDCl_3$, 100 MHz, ppm): δ 14.1, 22.7, 26.8, 27.5, 31.7, 52.4, 120.9, 121.1, 129.3, 148.2.

(6-Carbazol-9-yl-hexyl)diphenyl-amine (3) Carbazole (0.836 g, 5.0 mmol) was added to a suspension of KOH (0.336 g, 6.0 mmol) in DMSO (15 mL) under nitrogen. The mixture was stirred for 10 min after which time **1** (1.83 g, 5.5 mmol) was added. The reaction was stirred for 4 h at room temperature. Water was added and extracted with dichloromethane (3 × 30 mL), the organic phases were then washed with brine, dried with anhydrous sodium sulfate and evaporated. The residue was purified by chromatography on silica gel (dichloromethane: petroleum = 1: 20) to give **3** (1.84 g, 88.3%) as a colorless liquid. ^{1}H NMR ($CDCl_3$, 400 MHz, ppm): δ 1.37–1.38 (m, 4H), 1.59–1.66 (m, 2H), 1.82–1.89 (m, 2H), 3.64 (t, J = 7.6 Hz, 2H), 4.27 (t, J = 7.2 Hz, 2H), 6.91–6.96 (m, 6H), 7.21–7.25 (m, 6H), 7.36–7.38 (m, 2H), 7.43–7.47 (m, 2H), 8.09–8.11 (m, 2H). ^{13}C NMR ($CDCl_3$, 100 MHz, ppm): δ 26.8, 27.1, 27.3, 28.9, 42.8, 52.1, 108.6, 118.7, 120.3, 120.8, 121.0, 122.8, 125.5, 129.2, 140.3, 148.0. ESI MS: m/z 418.2. Found: 419.3 $[M + H]^+$. Anal. Calcd. for $C_{30}H_{30}N_2$: C, 86.08; H, 7.22; N, 6.69. Found: C, 85.89; H, 7.24; N, 6.72.

(6-Phenothiazin-10-yl-hexyl)diphenyl-amine (4). It was prepared as a colorless liquid in 94.7% yield from phenothiazine by the same procedure established for **3**. ^{1}H NMR ($CDCl_3$, 400 MHz, ppm): δ 1.31–1.39 (m, 2H), 1.40–1.47 (m, 2H), 1.61–1.68 (m, 2H), 1.74–1.82 (m, 2H), 3.65 (t, J = 7.6 Hz, 2H), 3.82 (t, J = 7.2 Hz, 2H), 6.82–6.84 (m, 2H), 6.88–6.96 (m, 8H), 7.11–7.15 (m, 4H), 7.22–7.24 (m, 4H). ^{13}C NMR ($CDCl_3$, 100 MHz, ppm): δ 26.6, 26.7, 26.8, 27.4, 47.1, 52.1, 115.3, 120.8, 121.0, 122.3, 124.9, 127.1, 127.4, 129.2, 145.2, 148.0. ESI MS: m/z 450.2. Found: 451.2 $[M + H]^+$. Anal. calcd. for $C_{30}H_{30}N_2S$: C, 79.96; H, 6.71; N, 6.22; S 7.12. Found: C, 79.71; H, 6.73; N, 6.24; S, 7.09.

9-{6-[(4-Formyl-phenyl)-phenyl-amino]-hexyl}-9*H*-carbazol-3-carbaldehyde (5). To a solution of **3** (1.67 g, 4.0 mmol) and dry DMF (1.76 g, 24 mmol) in ClC_2H_4Cl (15 mL), $POCl_3$ (3.69 g, 24 mmol) was added slowly at 0 °C. Then the bath was heated to 90 °C and maintained for 4 h. Dilute aqueous solution of NaOH was added and the mixture extracted with CH_2Cl_2. The organic fractions were washed with brine and dried over anhydrous sodium sulfate. The solvent was removed under reduced pressure and the residue was purified by chromatography on silica gel (dichloromethane: petroleum = 2: 1) to give **5** (1.61 g, 84.8%) as a pale-yellow liquid. ^{1}H NMR ($CDCl_3$, 400 MHz, ppm): δ 1.15–1.25 (m, 4H), 1.43–1.53 (m, 2H), 1.64–1.75 (m, 2H), 3.49 (t, J = 7.2 Hz, 2H), 4.09 (t, J = 6.4 Hz, 2H), 6.49–6.51 (m, 2H), 6.68–6.69 (m, 2H), 6.99–7.00 (m, 2H), 7.11–7.24 (m, 4H), 7.35–7.39 (m, 1H), 7.47–7.49 (m, 2H), 7.80–7.82 (m 1H), 7.95–7.97 (m,1H), 8.38–8.40 (m, 1H), 9.58(s, 1H), 9.90(s, 1H). ^{13}C NMR ($CDCl_3$, 100 MHz, ppm): δ 26.3, 26.7, 26.8, 28.5, 42.8, 52.0, 108.6, 109.1, 113.0, 114.3, 120.0, 120.4, 122.6, 123.6, 126.1, 126.2, 126.4, 126.7, 128.2, 129.8, 131.4, 140.7, 143.6, 145.2, 152.9, 153.4, 189.8, 191.3. ESI MS: m/z 474.2. Found: 475.2 $[M + H]^+$. Anal. Calcd. for $C_{32}H_{30}N_2O_2$: C, 80.98; H, 6.37; N, 5.90. Found: C, 81.14; H, 6.40; N, 5.87.

10-{6-[(4-Formyl-phenyl)-phenyl-amino]-hexyl}-10*H*-phenothiazin-3-carbaldehyde (6). It was prepared as a yellow liquid in 72.7% yield from **4** by the same procedure established for **5**. ^{1}H NMR ($CDCl_3$, 400 MHz, ppm): δ 1.32–1.39 (m, 2H), 1.42–1.49 (m, 2H), 1.64–1.68 (m, 2H), 1.76–1.83 (m, 2H), 3.68 (t, J = 7.6 Hz, 2H), 3.88 (t, J = 6.8 Hz, 2H), 6.64–6.67 (m, 2H), 6.84–6.88 (m, 2H), 6.95–6.97 (m, 1H), 7.10–7.17 (m, 4H), 7.28–7.30 (m, 1H), 7.40–7.44 (m, 2H), 7.58–7.65 (m, 4H), 9.72 (s, 1H), 9.78 (s, 1H). ^{13}C NMR ($CDCl_3$, 100 MHz, ppm): δ 26.3, 26.4, 26.5, 27.1, 47.5, 52.3, 113.2, 114.5, 114.8, 115.9, 123.6, 123.9, 125.2, 126.3, 127.4, 127.5, 128.3, 129.9, 130.0, 131.0, 131.6, 143.3, 145.5, 150.6, 153.2, 153.7, 189.9, 190.1. ESI MS: m/z 506.2. Found: 529.1 $[M + Na]^+$. Anal. Calcd. for $C_{32}H_{30}N_2O_2S$: C, 75.86; H, 5.97; N, 5.53; S, 6.33. Found: C, 75.67; H, 6.00; N, 5.55; S, 6.30.

4-(Hexyl-phenyl-amino)-benzaldehyde (7). It was prepared as a light yellow liquid in 77.8% yield from **2** by using the method established for **5.** ^{1}H NMR ($CDCl_3$, 400 MHz, ppm): δ 0.87 (t, J = 6.8 Hz, 3H), 1.28–1.37 (m, 6H), 1.65–1.72 (m, 2H), 3.71 (t, J = 8.0 Hz, 2H), 6.68–6.70 (m, 2H), 7.19–7.21 (m, 2H), 7.25–7.29 (m, 1H), 7.40–7.44 (m, 2H), 7.63–7.66 (m, 2H), 9.72 (s, 1H). ^{13}C NMR ($CDCl_3$, 100 MHz, ppm): δ 13.9, 22.5, 26.4, 27.22, 31.4, 52.5, 113.1, 126.2, 126.3, 127.4, 130.0, 131.6, 145.6, 153.2, 190.0. ESI MS: m/z 281.2. Found: 282.1 $[M + H]^+$. Anal. Calcd. for $C_{19}H_{23}NO$: C, 81.10; H, 8.24; N, 4.98. Found: C, 80.93; H, 8.27; N, 4.99.

(*E*)-3-[4-({6-[3-((*E*)-2-Cyano-2-thiophen-2-yl-vinyl)phenothiazin-10-yl]hexyl}phenyamino)phenyl]-2-thiophen-2-yl-acrylonitrile (8). To a stirred solution of t-BuOK (0.0224 g, 0.20 mmol) and 2-thiopheneacetonitrile (0.985 g, 8.0 mmol) in THF (20 mL), 6 (1.01 g, 2.0 mmol) was added at room temperature under nitrogen. The reaction mixture was refluxed for 2 h then cooled to room temperature then the mixture was concentrated under reduced pressure. The resulting residue was purified by chromatography on silica gel (ethyl acetate: petroleum = 1: 15) to give **8**

(1.18 g, 82.5%) as a scarlet liquid. ^{1}H NMR ($CDCl_3$, 400 MHz, ppm): δ 1.34–1.40 (m, 2H), 1.43–1.47 (m, 2H), 1.64–1.71 (m, 2H), 1.75–1.82 (m, 2H), 3.68 (t, J = 7.2 Hz, 2H), 3.84 (t, J = 6.8 Hz, 2H), 6.69–6.72 (m, 2H), 6.81–6.84 (m, 2H), 6.91–6.95 (m, 1H), 7.01–7.04 (m, 2H), 7.09–7.12 (m, 2H), 7.15–7.19 (m, 4H), 7.20–7.22 (m, 2H), 7.23–7.25 (m, 2H), 7.30–7.31 (m, 1H), 7.36–7.40 (m, 2H), 7.50 (s, 1H), 7.68–7.74 (m, 3H). ^{13}C NMR ($CDCl_3$, 100 MHz, ppm): δ 26.5, 26.6, 27.3, 29.7, 47.4, 52.2, 100.2, 103.2, 114.6, 115.2, 115.6, 117.2, 118.0, 122.8, 123.1, 123.9, 124.7, 125.0, 125.4, 125.5, 125.6, 126.5, 126.6, 127.4, 127.5, 127.6, 127.9, 128.0, 128.2, 128.3, 129.9, 130.8, 138.3, 139.5, 139.9, 140.3, 143.8, 146.0, 147.0, 150.1. ESI MS: m/z 716.2. Found: 739.3 $[M + Na]^+$. Anal. Calcd. for $C_{44}H_{36}N_4S_3$: C, 73.71; H, 5.06; N, 7.81; S, 13.42. Found: C, 73.59; H, 5.09; N, 7.85; S, 13.37.

(*E*)-3-[4-(Hexyl-phenyl-amino)-phenyl]-2-thiophen-2-yl-acrylonitrile (9). It was prepared as a yellow liquid in 87.8% yield from **7** by using the method established for **8.** ^{1}H NMR ($CDCl_3$, 400 MHz, ppm): δ 0.79 (t, J = 6.4 Hz, 3H), 1.17–1.26 (m, 6H), 1.55–1.62 (m, 2H), 3.61 (t, J = 8.0 Hz, 2H), 6.64–6.66 (m, 2H), 6.91–6.93 (m, 1H), 7.09–7.14 (m, 5H), 7.16–7.17 (m, 1H), 7.29–7.32 (m, 2H), 7.61–7.63 (m, 2H). ^{13}C NMR ($CDCl_3$, 100 MHz, ppm): δ 14.1, 22.7, 26.8, 27.4, 31.7, 52.6, 100.3, 114.7, 118.1, 122.8, 124.8, 125.5, 125.6, 126.8, 128.0, 130.0, 130.9, 140.1, 140.5, 146.3, 150.3. ESI MS: m/z 386.2. Found: 387.1 $[M + H]^+$. Anal. Calcd. for $C_{25}H_{26}N_2S$: C, 77.68; H, 6.78; N, 7.25; S, 8.30. Found: C, 77.58; H, 6.80; N, 7.26; S, 8.29.

(*E*)-3-{4-[(6-{3-[(*E*)-2-Cyano-2-(5-formylthiophen-2-yl) vinyl]phenothiazin-10-yl} hexyl)phenylamino]phenyl}-2-(5-formylthiophen-2-yl)acrylonitrile (10). It was prepared as a red-black solid in 66.7% yield from **8** by the same procedure established for **5**, mp 90–91 °C. ^{1}H NMR ($CDCl_3$, 400 MHz, ppm): δ 1.37–1.43 (m, 2H), 1.44–1.52 (m, 2H), 1.67–1.74 (m, 2H), 1.76–1.83 (m, 2H), 3.79 (t, J = 7.2 Hz, 2H), 3.89 (t, J = 6.4 Hz, 2H), 6.84–6.86 (m, 2H), 6.95–6.97 (m, 2H), 7.05–7.14 (m, 3H), 7.17–7.19 (m, 2H), 7.29–7.32 (m, 2H), 7.36–7.40 (m, 3H), 7.58 (s, 1H), 7.69–7.70 (m, 1H), 7.72–7.74 (m, 2H), 7.78–7.80 (m, 1H), 7.83–7.86 (m, 2H), 9.81(s, 1H), 9.86 (s, 1H). ^{13}C NMR ($CDCl_3$, 100 MHz, ppm): δ 26.4, 26.5, 26.6, 27.4, 47.4, 52.1, 101.9, 104.6, 115.2, 115.8, 116.5, 117.1, 117.3, 123.5, 123.7, 124.0, 125.2, 126.0, 126.7, 126.8, 126.9, 127.5, 127.6, 128.1, 128.6, 128.7, 129.0, 129.4, 130.7, 131.6, 136.9, 138.5, 139.3, 141.6, 142.5, 143.4, 147.8, 148.1, 148.7, 152.2, 182.4, 190.3. ESI MS: m/z 772.2. Found: 773.1 $[M + H]^+$. Anal. Calcd. for $C_{46}H_{36}N_4O_2S_3$: C, 71.47; H, 4.69; N, 7.25; S, 12.44. Found: C, 71.68; H, 4.71; N, 7.24; S, 12.42.

(*E*)-2-(5-Formyl-thiophen-2-yl)-3-[4-(hexyl-phenyl-amino)-phenyl]acrylonitrile (11). It was prepared as a red liquid in 79.4% yield from **9** by using the method established for **5**. ^{1}H NMR ($CDCl_3$, 400 MHz, ppm): δ 0.80 (t, J = 6.4 Hz, 3H), 1.18 (br. s, 6H), 1.59–1.64 (m, 2H), 3.65 (t, J = 8.0 Hz, 2H), 6.63–6.65 (m, 2H), 7.13–7.15 (m, 2H), 7.19–7.25 (m, 2H), 7.32 (s, 1H); 7.35–7.38 (m, 2H), 7.60–7.61 (m, 1H), 7.69–7.71 (m, 2H), 9.77 (s, 1H). ^{13}C NMR ($CDCl_3$, 100 MHz, ppm): δ 14.0, 22.6, 26.7, 27.3, 31.6, 52.7, 98.4, 114.1, 117.4, 121.7, 125.6, 126.4, 127.3, 130.1, 131.9, 137.2, 141.6, 143.3, 145.7, 150.3, 151.3, 182.4. ESI MS: m/z 414.2. Found: 415.2 $[M + H]^+$. Anal. Calcd. for $C_{26}H_{26}N_2OS$: C, 75.33; H, 6.32; N, 6.76; S, 7.73. Found: C, 75.31; H, 6.34; N, 6.77; S, 7.74.

(*E*)-3-[4-({6-[3-((*E*)-2-Carboxy-2-cyanovinyl)carbazol-9-yl]-hexyl}phenylaminophenyl]-2-cyanoacrylic acid (DC1). 5 (0.379 g, 0.80 mmol) dissolved in $CHCl_3$ (15 mL) was condensed with 2-cyanoacetic acid (0.680 g, 8.0 mmol) in the presence of piperidine (0.32 mL, 3.2 mmol). The mixture was refluxed for 3 h under nitrogen. After cooling, the mixture was poured into a mixture of CH_2Cl_2 and 2 M aqueous HCl. The organic layer was separated and dried over anhydrous sodium sulfate. After removal of the solvent at reduced pressure, the crude product was purified by chromatography on silica gel (methylene chloride: methanol: acetic acid = 100: 5: 1) to give **DC1** as a yellow solid (0.366 g, 75.3%). mp 168–169 °C. ^{1}H NMR (DMSO-d_6, 400 MHz, ppm): δ 1.15 ~ 1.27 (m, 4H), 1.45 (br. s, 2H), 1.70 (br. s, 2H), 3.62 (br. s, 2H), 4.36 (br. s, 2H), 6.62–7.64 (m, 2H), 7.17–7.27 (m, 4H); 7.41–7.61 (m, 4H), 7.69–7.71 (m, 1H), 7.80–7.82 (m, 2H), 8.01 (s, 1H), 8.10–8.11 (m, 1H), 8.21–8.23 (m, 1H), 8.40 (s, 1H), 8.78 (s, 1H). ^{13}C NMR (DMSO-d_6, 100 MHz, ppm): δ 25.8, 26.1, 26.6, 28.3, 42.5, 51.6, 95.8, 99.4, 110.1, 113.5, 117.6, 117.6, 117.7, 120.1, 120.3, 120.5, 122.0, 122.5, 125.3, 126.5, 126.8, 126.9, 127.1, 127.7, 130.1, 133.2, 140.7, 142.5, 144.7, 151.9, 153.2, 154.6, 164.3, 164.6. ESI MS: m/z 608.2. Found: 606.9 $[M-H]^-$. Anal. Calcd. for $C_{38}H_{32}N_4O_4$: C, 74.98; H, 5.30; N, 9.20. Found: C, 74.79; H, 5.27; N, 9.17.

(*E*)-3-[4-({6-[3-((*E*)-2-Carboxy-2-cyanovinyl)phenothiazin-10-yl]-hexyl}-phenylamino)phenyl]-2-cyanoacrylic acid (DC2). It was prepared as a black solid in 62.1% yield from **6** by the same procedure established for **DC1**, mp 230–231 °C. ^{1}H NMR (DMSO-d_6, 400 MHz, ppm): δ 1.28–1.40 (m, 4H), 1.50–1.58 (m, 2H), 1.61–1.68 (m, 2H), 3.70 (t, J = 6.8 Hz, 2H), 3.90 (t, J = 6.0 Hz, 2H), 6.68–6.70 (m, 2H), 6.96–6.99 (m, 1H), 7.03–7.05 (m, 1H), 7.10–7.14 (m, 2H), 7.11–7.19 (m, 1H), 7.21–7.23 (m, 2H), 7.28–7.31 (m, 1H), 7.43–7.47 (m, 2H), 7.76 (s, 1H), 7.83–7.85 (m, 3H), 8.03 (s, 1H), 8.06 (s, 1H). ^{13}C NMR (DMSO-d_6, 100 MHz, ppm): δ 25.8, 25.8, 26.0, 26.9, 46.8, 51.7, 99.2, 105.2, 113.8, 115.8, 116.5, 118.3, 118.6, 120.7, 122.4, 123.5, 123.6, 126.4, 127.1, 127.4, 128.1, 128.4, 130.3, 130.9, 132.8, 143.2, 145.1, 148.0, 149.8, 151.6, 151.9, 154.22, 165.1, 165.7. ESI MS: m/z 640.2. Found: 639.3 $[M-H]^-$. Anal. Calcd. for $C_{38}H_{32}N_4O_4S$: C, 71.23; H, 5.03; N, 8.74; S, 5.00. Found: C, 71.17; H, 5.01; N, 8.73; S, 4.98.

(*E*)-3-{5-[(*E*)-2-(4-{[6-(3-{(*E*)-2-[5-((*E*)-2-Carboxy-2-cyanovinyl)thiophen-2-yl]-2-cyanovinyl}phenothiazin-10-yl)-hexyl]phenylamino}phenyl)-1-cyanovinyl]thiophen-2-yl}-2-cyanoacrylic acid (DC3). It was prepared as a black solid in 64.6% yield from **10** by the same procedure established for **DC1**, mp 126–128 °C. ^{1}H NMR (DMSO-d_6, 400 MHz, ppm): δ 1.36 (br. s, 4H), 1.55 (br. s, 2H), 1.65 (br. s, 2H), 3.79 (br. s, 2H), 3.88 (br. s, 2H), 6.94–7.08 (m, 5H), 7.11–7.22 (m, 5H), 7.37 (br. s, 1H), 7.44 (br. s, 1H), 7.62–7.80 (m, 6H), 7.82–7.96 (m, 4H), 8.01 (s, 1H), 8.17 (s, 1H). ^{13}C NMR (DMSO-d_6, 100 MHz, ppm): δ 25.6, 25.6, 25.8, 26.9, 46.6, 51.3, 100.9, 102.2, 115.7, 116.3, 117.0, 117.4, 118.3, 118.4, 118.7, 122.2, 122.4, 123.3, 124.3, 126.1, 126.3, 127.1, 127.3, 127.7, 127.9, 128.4, 129.8, 130.7, 131.3, 131.3, 132.1, 132.2, 136.7, 136.9, 138.8, 139.4, 141.0, 141.5, 141.6, 141.6, 143.0, 144.4, 147.2, 147.7, 149.8, 150.5, 163.2, 164.4. ESI MS: m/z 906.2. Found: 905.0 $[M-H]^-$. Anal. Calcd. for $C_{52}H_{38}N_6O_4S_3$: C, 68.85; H, 4.22; N, 9.26; S, 10.60. Found: C, 68.72; H, 4.19; N, 9.26; 10.30.

(*E*)-2-Cyano-3-(5-{(*E*)-1-cyano-2-[4-(hexyl-phenyl-amino)-phenyl]vinyl}-thiophen-2-yl)-acrylic acid (SC). It was prepared as a black solid in 79.2% yield from **11** by using the method established for **DC1**, mp 73–74 °C ^{1}H NMR (DMSO-d_6, 400 MHz, ppm): δ 0.82 (t, J = 6.4 Hz, 3H), 1.21–1.24 (m, 4H), 1.28–1.32 (m, 2H), 1.54–1.62 (m, 2H), 3.75 (t, J = 7.8 Hz, 2H), 6.75–6.78 (m, 2H), 7.26–7.28 (m, 2H), 7.29–7.31 (m, 1H), 7.45–7.7.51 (m, 3H), 7.79 (s, 1H), 7.83–7.85 (m, 2H), 7.93–7.94 (m, 1H), 8.42 (s, 1H). ^{13}C NMR (DMSO-d_6, 100 MHz, ppm): δ 13.9, 22.1, 25.9, 26.9, 31.1, 51.8, 96.8, 99.1, 114.0, 116.7, 117.7, 121.6, 125.2, 126.3, 127.0, 130.2, 132.0, 134.4, 140.9, 143.6, 145.2, 145.9, 148.9, 151.1, 163.6. ESI MS: m/z 481.1. Found, 435.7 $[M-COOH]^-$. Anal. Calcd. for $C_{29}H_{27}N_3O_2S$: C, 72.32; H, 5.65; N, 8.72; S, 6.66. Found: C, 72.39; H, 5.67; N, 8.73; S, 6.65.

2.3. Fabrication of DSSCs

The paste fabrication process of the TiO_2 (20 nm particle size) screen-printed FTO coated glass (15 Ω/square, Nippon Sheet Glass, Japan) was carried out according to the previous paper [24]. Briefly, TiO_2 powder (20 nm) (1.0 g) was ground for 40 min in the mixture of ethanol (8.0 mL), acetic acid (0.2 mL), terpineol

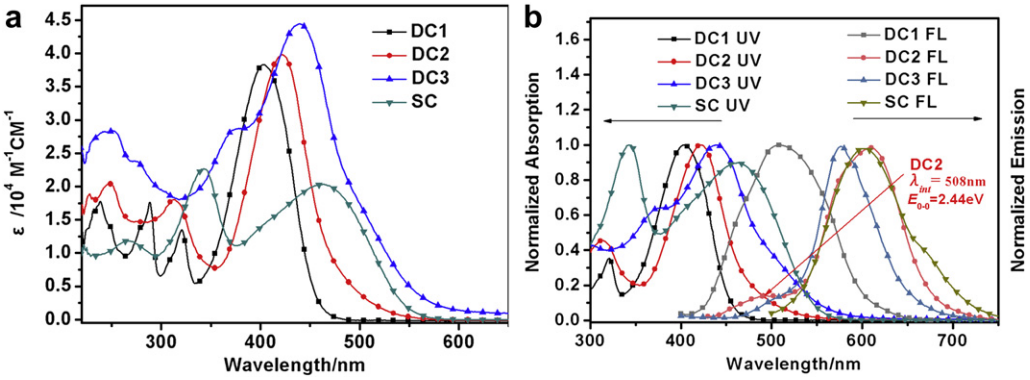

Fig. 1. (a) Absorption spectra and (b) Normalized absorption and emission spectra of the dyes in CH_2Cl_2/MeOH.

(3.0 g) and ethyl cellulose (0.5 g) to form a slurry, and then the slurry was sonicated for 5 min in an ultrasonic bath, finally to form a viscous white TiO_2 paste. The thickness of films was controlled through repeating screen-printing times. After a heating process (at 325 °C for 5 min, at 375 °C for 5 min, at 450 °C for 15 min, and then at 500 °C for 15 min) to remove the organic substances, the TiO_2 films were soaked in 0.04 M $TiCl_4$ aqueous solution for 30 min at 70 °C to improve the photovoltaic performance. After sintering at 520 °C for 30 min, the TiO_2 electrode films were immerged into 0.2 mM dye (**DC1**, **DC2**, **DC3** and **SC**) in CH_3OH/CH_2Cl_2 (1:1; v/v), and sensitized for about 15 h at room temperature. Afterward, these films were rinsed with CH_2Cl_2 in order to remove physisorbed organic dye molecule. To evaluate their photovoltaic performance, the dye-sensitized TiO_2/FTO glass films were sandwiched together with Pt coated FTO glass which was used as counter electrode. Platinized counter electrodes were fabricated by thermal depositing H_2PtCl_6 solution (5 mM in isopropanol) onto FTO glass. Then the counter electrode was placed directly on the top of the dye-sensitized TiO_2 film sealed with thermal adhesive film (~25 μm). The electrolyte (0.6 M 1-methyl-3-propylimidazolium iodide (PMII), 0.10 M guanidinium thiocyanate, 0.03 M I_2, 0.5 M tert-butylpyridine in acetonitrile and valeronitrile (85:15)) was injected from a hole made on the counter electrode into the space between the sandwiched cells.

3. Result and discussion

3.1. Synthesis and structural characterization

The synthetic route of the dyes is shown in Scheme 1. Intermediate **1** or **2** was prepared from diphenylamine via alkylation reaction with 1,6-dibromohexane or 1-bromohexane, respectively. Compound **1** followed further alkylation with carbazole and phenothiazine in the presence of KOH in DMSO to afford compounds **3** and **4**, respectively. The intermediates **3**, **4** and **2** were then converted to the corresponding dialdehydes **5**, **6** and aldehyde **7** by Vilsmeier–Haack reaction in the presence of DMF and $POCl_3$. **8** and **9** were obtained via Knoevenagel reaction of the **6** and **7** with 2-thiopheneacetonitrile in THF. The dialdehyde **10** and aldehyde **11** were also prepared by a similar process to **5**. Finally, the dialdehydes **5**, **6**, **10** and the aldehyde **11** were condensed with cyanoacetic acid to yield the target dyes (**DC1**, **DC2**, **DC3** and **SC**) by the Knoevenagel reaction in refluxing $CHCl_3$ in the presence of piperidine. All the intermediates and target dyes were confirmed by standard spectroscopic methods.

3.2. Photophysical properties

The UV–vis and emission spectra of the dyes in CH_2Cl_2/MeOH (1:1) solution and the absorption spectra of the dyes on TiO_2 films are shown in Fig. 1 and Fig. 2, respectively, and the characteristic data are presented in Table 1. All the dyes exhibit two distinct absorption bands appearing at 320–390 nm and 400–600 nm, respectively. The former is ascribed to a localized aromatic π–π* transition and the later is assigned to the intramolecular charge transfer (ICT) between donor and acceptor. Compared to **DC1**, **DC2** possesses a broader absorption near to 550 nm and the absorption maximum is red-shift by 19 nm, which is due to the stronger electron-donating ability of phenothiazine than that of carbazole [25]. It is interesting to note that when the π-bridge of vinylthiophene is introduced into each chain of **DC2**, the resulting product **DC3** exhibits a broaden and more intensive absorption compared to **DC2**, and a shoulder can be observed clearly near 490 nm of **DC3** which perhaps is attributed to the absorption overlap and complement of the donors and thiophene spacers in the two independent D–π–A units. The overlap and complement in the absorption of **DC2** or **DC1** are not observed apparently. However, the molar absorption coefficient ($\varepsilon = 39{,}823\ M^{-1}\ cm^{-1}$) of **DC2** is much higher than that of compound **SB** with single chain ($\varepsilon = 16{,}000\ M^{-1}\ cm^{-1}$) [14], which indicates that the absorption of the dyes is enhanced by double D–π–A systems in one molecule. The above phenomenons can also be observed clearly from the

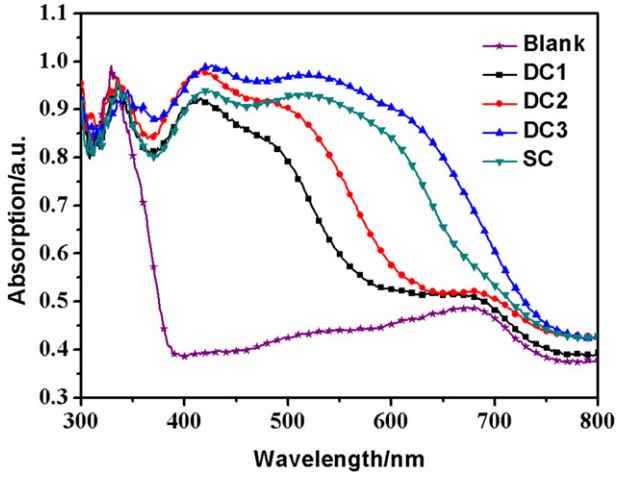

Fig. 2. Absorption spectra of the dyes anchored on TiO_2 films.

Table 1
Absorption, emission and electrochemical properties of the dyes **DC1**, **DC2, DC3** and **SC**.

Dye	Absorption		Emission	Oxidation potential data					E_{HOMO}/E_{LUMO}[b]/eV
	λ_{max}/nm	ε/M^{-1} cm^{-1}	λ_{max}/nm	E_{ox}/V (vs NHE)	E_{0-0}/V	$E_{ox} - E_{0-0}$/V (vs.NHE)	E_{gap}[a]/V (vs NHE)	E_{HOMO}/E_{LUMO}/eV	
DC1	321	15,599	509 (403)	0.92	2.79	−1.87	1.37	−5.17/−2.38	−5.90/−2.29[c]
	403	38,289							−5.63/−2.15[d]
DC2	321	18,030	610 (422)	0.99	2.44	−1.45	0.95	−5.24/−2.80	−5.61/−2.12[d]
	422	39,823							−5.47/−2.50[e]
DC3	382	28,760	576 (439)	0.93	2.34	−1.41	0.91	−5.18/−2.84	−5.44/−2.75[d]
	439	44,447							−5.41/−2.99[e]
SC	343	22,633	599 (463)	0.96	2.31	−1.35	0.85	−5.21/−2.90	−5.33/−2.75[d]
	463	20,311							

[a] E_{gap} is the energy gap between the $E_{ox} - E_{0-0}$ of the dye and the conductive band level of TiO_2 (−0.5 V vs NHE).
[b] Calculated at the B3LYP-31G(d) level in vacuum.
[c] Calculated HOMO–LUMO levels for the chain of **DC1** which employed carbazole as donor.
[d] Calculated HOMO–LUMO levels for the chain of **DC1, DC2**, **DC3** and **SC** which employed diphenylamine as donor.
[e] Calculated HOMO–LUMO levels for the chain of **DC2** and **DC3** which employed phenothiazine as donor.

absorption of **DC3** and **SC**. It is obvious that the absorption of the dye **DC3** exhibited broaden and more intensive than that of **SC**. The absorption properties of the three dyes in the solution are consistent with the energy optical band (E_{0-0}) between the HOMO and LUMO energy levels, and can also be proved by the molecular optimization results of the dyes (Fig. 3). Compared to the absorption spectra of the dyes in the solution, the absorption spectra on TiO_2 (Fig. 2) are broadened, and the absorption intensity in the ultraviolet region decreases; however, the absorption intensity in the visible light region increases, accompanying with a bathochromic shift of the absorption maximum [26].

3.3. Electrochemical properties

To evaluate the feasibility of the regeneration of the dyes and electron injection from the excited state of the dyes to the conduction band (CB) of TiO_2, the electrochemical behavior of the dyes was studied by cyclic voltammetry (CV) (Table 1). The first half-wave potentials ($E_{1/2}$ vs. Fc/Fc^+) of **DC1**, **DC2 DC3** and **SC** adsorbed on TiO_2 film were determined to be 0.29, 0.36, 0.30 and 0.33 V, respectively. Therefore, the first oxidation potentials (E_{ox}) versus normal hydrogen electrode (NHE), corresponding to the highest occupied molecular orbital (HOMO) levels, were 0.92, 0.99, 0.93 and 0.96 V calibrated by addition of 0.63 V to the potential vs Fc/Fc^+ (vs NHE), respectively. The estimated excited state potentials corresponding to the lowest unoccupied molecular orbital (LUMO) levels, were −1.87, −1.45, −1.41 and −1.33 V (vs NHE) calculated from $E_{ox} - E_{0-0}$, where the E_{0-0} were calculated from intersection of the normalized absorption and the emission spectra (λ_{int}) and $E_{0-0} = 1240/\lambda_{int}$ (Fig. 1b). On the other hand, the HOMO values versus vacuum were transformed via the equation $E_{HOMO} = -e[4.88 + E_{1/2}\,(\text{vs. } Fc/Fc^+)]$ [27], and the corresponding E_{HOMO} of **DC1-**

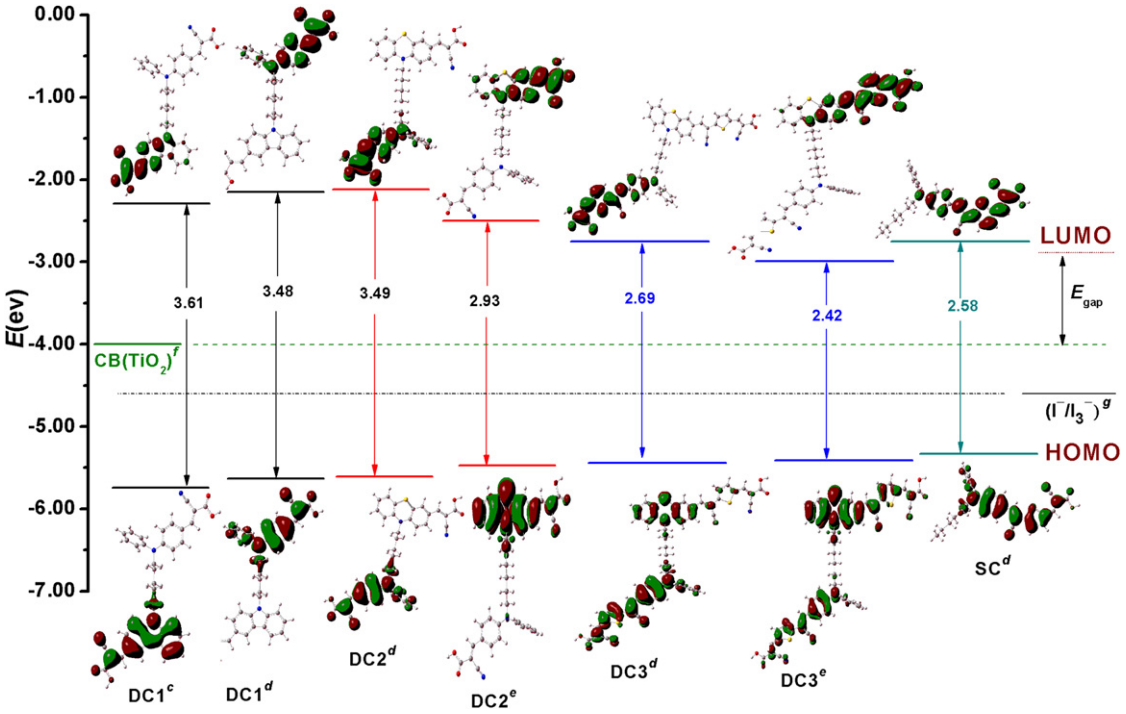

Fig. 3. The optimized structure and the frontier molecular orbitals of the HOMO and LUMO calculated with DFT on a B3LYP/6−31 + G(d) level of the dyes. c: Calculated HOMO-LUMO levels for the chain of **DC1** which employed carbazole as donor; d; Calculated HOMO-LUMO levels for the chain of **DC1**, **DC2**, **DC3** and **SC** which employed diphenylamine as donor; e: Calculated HOMO-LUMO levels for the chain of **DC2** and **DC3** which employed phenothiazine as donor; f: Energy level of the conduction band edge of TiO2 (−4.00 eV vs vacuum) [29]; g: Energy level of the I3-/I- redox couple (−4.60 eV vs vacuum) [28].

3 and **SC** versus vacuum were −5.17, −5.24, −5.18 and −5.21 eV, respectively. The E_{LUMO} calculated by [E_{HOMO} + E_{0-0}] were −2.38, −2.80, −2.84 and −2.90 eV, respectively. The results showed that the HOMO levels of all the dyes were sufficiently higher than that of I^-/I_3^- redox potential value (0.4 V vs NHE or −4.60 eV vs vacuum) [28], indicating that the oxidized dyes formed after electron injection into the CB of TiO_2 could thermodynamically accept electrons from I^- ions and then were regenerated. The LUMO levels of these dyes were significantly lower than that of the conduction band edge energy level of the TiO_2 electrode (−0.5 V vs NHE or −4.00 eV vs vacuum) [29], and provided that an energy gap (E_{gap}) of 0.2 eV [30] was necessary for efficient electron injection. Hence, an effective electron transfer from the excited dye to TiO_2 was ensured.

3.4. Molecular orbital calculations

To gain an insight into the molecular structure and electron distribution, density functional theory (DFT) calculations were performed on a B3LYP/6−31 + G (d) level with Gaussian 03. The electron distributions of the HOMO and LUMO of the dyes are shown in Fig. 3. At the ground state for all the dyes, electrons are homogeneously distributed in both the donors (diphenylamine, carbazole and phenothiazine) and π-bridge, and upon the light illumination, electrons move from the HOMO to the LUMO by an intramolecular charge transfer, and are finally located in anchoring groups through the π-bridge. The results indicated that the high electron density from the donor units moved to the cyanoacrylic acid moieties in the HOMO−LUMO excitation induced by light, thus allowing an efficient photoinduced electron transfer from the dye to the TiO_2 electrode.

3.5. Photovoltaic performances of the DSSCs

The current−voltage (J−V) curves of DSSCs based on **DC1**-**3** and **SC** are shown in Fig. 4. The detailed parameters of short-circuit current density (J_{sc}), open-circuit voltage (V_{oc}), fill factor (FF) and overall conversion efficiency (η) are summarized in Table 2. Among these dyes, the cell based on **DC3** exhibited a maximum η of 5.19% (J_{sc} = 10.79 mA cm^{-2}, V_{oc} = 687 mV, FF = 0.70) under standard global AG 1.5G solar light irradiation (100 mW cm^{-2}). Under the same measuring conditions, while the cells sensitized with **DC2**, **DC1** and **SC** gave J_{sc} of 8.98, 5.73 and 8.20 mA cm^{-2}, V_{oc} of 756, 715 and 655 mV and FF of 0.69, 0.69 and 0.71, corresponding to η of 4.66, 2.82 and 3.80%, respectively. The highest η of the cell based on **DC3** due to its relatively higher J_{sc}, which could be ascribed to its higher light harvesting efficiency in the visible region.

Table 2
Photovoltaic parameters of DSSCs.

Dye	J_{sc}/mA cm^{-2}	V_{oc}/mV	FF	η/%
DC1	5.73	715	0.69	2.82
DC2	8.98	756	0.69	4.66
DC3	10.79	687	0.70	5.19
SC	8.20	655	0.71	3.80

The incident monochromatic photon-to-current conversion efficiency (IPCE) spectra of the DSSCs are plotted in Fig. 5. For **DC3** based cell, a high IPCE (above 50%) was obtained in the range from 400 to 560 nm with a maximum value of 68% at 480 nm, and the onset of IPCE tails off toward 705 nm. In the cases of **DC2**, **DC1** and **SC**, the IPCE exceeded 50% in a relatively narrow range of 400−523 nm, 400−467 nm and 435−532 nm and reached their maximum of 68% at 450 nm (for **DC2**), 63% at 401 nm (for **DC1**) and 59% at 469 nm (for **SC**), respectively. On the other hand, the onset of IPCE for **DC2, DC1** and **SC** was extended to 623 nm, 534 nm and 653 nm, which corresponds to blue-shifts of 82 nm, 171 nm and 52 nm, compared to **DC3,** respectively. The higher IPCE values for **DC3** based DSSC should be attributed to its broader absorption and enhanced molar extinction coefficient in the visible region, which matched well with the absorbance spectra of the dyes in solution. The higher and broader IPCE of the cell based on **DC3** could lead to a higher short-circuit photocurrent density (Table 2).

DC3 based cell exhibited a higher J_{sc} but lower V_{oc} value compared to that of **DC2** sensitized cell. In general, the V_{oc} value is quite sensitive to the electron lifetime in the conduction band of TiO_2 [31]. To further shed light on the difference in V_{oc} among the dyes sensitized solar cells, the electrochemical impedance spectroscopy (EIS) of the DSSCs based on different dyes were measured in the dark under a forward bias of −0.7 V. As shown in Fig. 6, two semicircles were observed in the Nyquist plots. The smaller and larger semicircles in the Nyquist plots were attributed to the charge transfer at the counter electrode/electrolyte interface and the TiO_2/dye/electrolyte interface, respectively. As shown in Fig. 6a, the radius of the larger semicircle was decreased gradually in the order of **DC2**, **DC1**, **SC** and **DC3** cell, which may result in the longest electron lifetime of **DC2** and shortest lifetime of **DC3**. Seemingly there will be a different conclusion compared to IMVS. However, according to the impedance parameters fitted by the equivalent

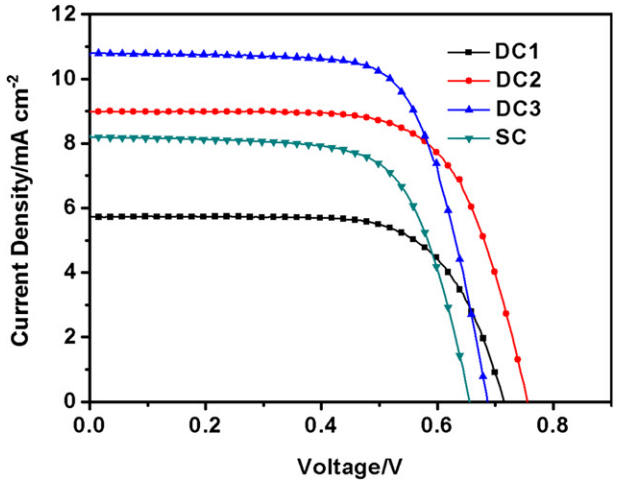

Fig. 4. J−V curves of DSSCs sensitized by **DC1**, **DC2**, **DC3** and **SC**.

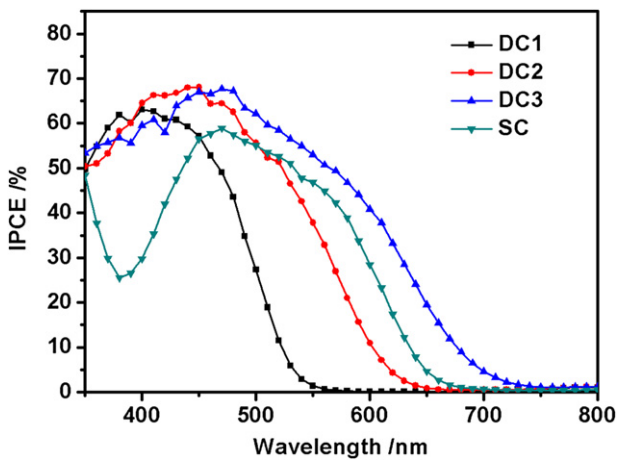

Fig. 5. IPCE spectra of DSSCs based on varied dyes.

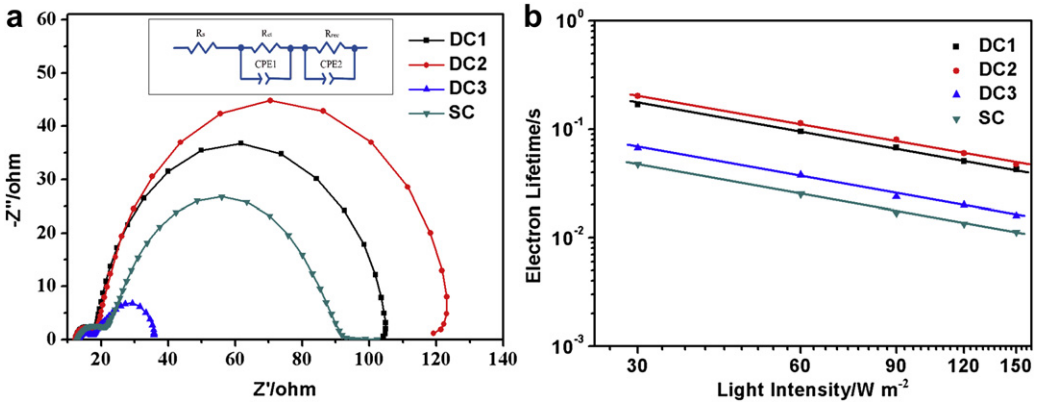

Fig. 6. Electrochemical impedance spectra (a) measured in the dark and electron lifetime (b) Incident light intensity dependent electron lifetime measured at 457 nm LED illumination for DSSCs sensitized by **DC1**, **DC2**, **DC3** and **SC**, respectively.

Table 3
Electrochemical parameters of DSSCs.

Dye	C/F (10^{-3})	R/Ω	Electron Lifetime/ms
DC1	1.14	87.25	99.7
DC2	1.37	107.1	146.7
DC3	5.37	17.35	93.2
SC	0.42	69.4	29.1

circuit (inset in Fig. 6a) with the fitted values listed in Table 2, where the electron lifetime can be estimated by $\tau_n = R_{rec} \times CPE2$ (CPE2: chemical capacitance) [32,33]. **DC3** based cell exhibits a smaller recombination resistance (R_{rec}) compared to **SC** based cell; however, the value of chemical capacitance (CPE2) of the DSSC based on **DC3** is larger. As a result, the electron lifetimes (τ_n) of DSSCs calculated by EIS showed the same order as the IMVS outcomes, although these values are usually larger than those obtained from IMVS, since the EIS measurement was performed in the dark. Hence, the electron lifetime values were in the order of **DC2** > **DC1** > **DC3** > **SC** implying the order of V_{oc} of **DC2** > **DC1** > **DC3** > **SC**. The results were in good agreement with those of the electron lifetime values calculated by the Nyquist curves (Table 3) and the V_{oc} values resolved by experiment (Table 2). Compared to the **DC** series dyes, the cell based on **SC** exhibited the shortest lifetime due to the lowest chemical capacitance, which resulted in the lowest V_{oc}.

4. Conclusion

In summary, a novel class of organic sensitizers (**DC1**-**DC3**) with two asymmetric D−π−A chains and a reference dye with a single D−π−A chain (**SC**) have been synthesized and characterized. Diphenylamine, carbazole and phenothiazine were used as electron donors, and cyanoacrylic acid was chosen as electron acceptor, Relatively high molar extinction coefficient of the **DC** series dyes were observed in the absorption maxima, which indicates that the complementary absorptions of the two independent D−π−A units have some overlap. Furthermore, absorption, electrochemical properties and photocurrent response of the dyes are sensitive to the electron-donating ability of the different donors and to the bridging linker. Among these dyes, the DSSC based on **DC3** exhibited the best overall light to electricity conversion efficiency of 5.19% (J_{sc} = 10.79 mA cm^{-2}, V_{oc} = 687 mV, FF = 0.70) under standard global AM 1.5 solar light irradiation (100 mW cm^{-2}). Compared to **DC2**, **DC1** and **SC**, the cell based on **DC3** had the higher η because of its relatively higher J_{sc}.

Acknowledgments

This work was financially supported by the National Natural Science Foundation of China (20872038, 20873183, 21072064), Jiangxi Province Natural Science Foundation of China (2009GQC0055) and the Natural Science Foundation of Guangdong Province, China (10351064101000000).

References

[1] Clifford JN, Martinez-Ferrero E, Viterisi A, Palomares E. Sensitizer molecular structure-device efficiency relationship in dye sensitized solar cells. Chem Soc Rev 2011;40:1635–46.
[2] O'Regan B, Grätzel M. A low-cost, high-efficiency solar cell based on dye-sensitized colloidal titanium dioxide films. Nature 1991;353:737–40.
[3] Yella A, Lee H-W, Tsao HN, Yi C, Chandiran AK, Nazeeruddin MK, et al. Porphyrin-sensitized solar cells with cobalt (II/III)–based redox electrolyte exceed 12 percent efficiency. Science 2011;334:629–34.
[4] Lee DH, Lee MJ, Song HM, Song BJ, Seo KD, Pastore M, et al. Organic dyes incorporating low-band-gap chromophores based on π-extended benzothiadiazole for dye-sensitized solar cells. Dyes Pigm 2011;91:192–8.
[5] Koumura N, Wang ZS, Mori S, Miyashita M, Suzuki E, Hara K. Alkyl-functionalized organic dyes for efficient molecular photovoltaics. J Am Chem Soc 2006;128:14256–7.
[6] Wang Z, Cui Y, Dan-Oh Y, Kasada C, Shinpo A, Hara K. Molecular design of coumarin dyes for stable and efficient organic dye-sensitized solar cells. J Phys Chem C 2008;112:17011–7.
[7] Kuang D-B, Uchida S, Humphry-Baker R, Zakeeruddin SM, Grätzel M. Organic dye-sensitized ionic liquid based solar cells: remarkable enhancement in performance through molecular design of indoline sensitizers. Angew Chem Int Ed 2008;47:1923–7.
[8] Hagberg DP, Yum J-H, Lee H, De Angelis F, Marinado T, Karlsson KM, et al. Molecular engineering of organic sensitizers for dye-sensitized solar cell applications. J Am Chem Soc 2008;130:6259–66.
[9] Chen R, Yang X, Tian H, Wang X, Hagfeldt A, Sun L. Effect of tetrahydroquinoline dyes structure on the performance of organic dye-sensitized solar cells. Chem Mater 2007;19:4007–15.
[10] Choi H, Baik C, Kang SO, Ko J, Kang MS, Nazeeruddin MK, et al. Highly efficient and thermally stable organic sensitizers for solvent-free dye-sensitized solar cells. Angew Chem Int Ed 2008;47:327–30.
[11] Maeda T, Nakao H, Kito H, Ichinose H, Yagi S, Nakazumi H. Far-red absorbing squarylium dyes with terminally connected electron-accepting units for organic dye-sensitized solar cells. Dyes Pigm 2011;90:275–83.
[12] Tian H, Yang X, Cong J, Chen R, Teng C, Liu J, et al. Effect of different electron donating groups on the performance of dye-sensitized solar cells. Dyes Pigm 2010;84:62–8.
[13] Wonneberger H, Pschirer N, Bruder I, Schöneboom J, Ma C-Q, Erk P, et al. Double donor-thiophene dendron-perylene monoimide: efficient light-harvesting metal-free chromophore for solid-state dye-sensitized solar cells. Chem – Asian J 2011;6:1744–7.
[14] Cao D, Peng J, Hong Y, Fang X, Wang L, Meier H. Enhanced performance of the dye-sensitized solar cells with phenothiazine-based dyes containing double D–A branches. Org Lett 2011;13:1610–3.
[15] Hong Y, Liao J-Y, Cao D, Zang X, Kuang D-B, Wang L, et al. Organic dye bearing asymmetric double donor-π-acceptor chains for dye-sensitized solar cells. J Org Chem 2011;76:8015–21.

[16] Tang J, Hua J, Wu W, Li J, Jin Z, Long Y, et al. New starburst sensitizer with carbazole antennas for efficient and stable dye-sensitized solar cells. Energy Environ Sci 2010;3:1736–45.
[17] Wu W, Yang J, Hua J, Tang J, Zhang L, Long Y, et al. Efficient and stable dye-sensitized solar cells based on phenothiazine sensitizers with thiophene units. J Mater Chem 2010;20:1772–9.
[18] Ooyama Y, Harima Y. Molecular designs and syntheses of organic dyes for dye-sensitized solar cells. Eur J Org Chem; 2009:2903–34.
[19] Chen Z, Li F, Huang C. Organic D-π-A dyes for dye-sensitized solar cell. Curr Org Chem 2007;11:1241–58.
[20] Fischer MKR, Wenger S, Wang MK, Mishra A, Zakeeruddin SM, Grätzel M, et al. D-π-A sensitizers for dye-sensitized solar cells: linear vs branched oligothiophenes. Chem Mater 2010;22:1836–45.
[21] Hagberg DP, Marinado T, Karlsson KM, Nonomura K, Qin P, Boschloo G, et al. Tuning the HOMO and LUMO energy levels of organic chromophores for dye sensitized solar cells. J Org Chem 2007;72:9550–6.
[22] Ito S, Miura H, Uchida S, Takata M, Sumioka K, Liska P, et al. High-conversion-efficiency organic dye-sensitized solar cells with a novel indoline dye. Chem Comm; 2008:5194–6.
[23] Wang Z-S, Koumura N, Cui Y, Takahashi M, Sekiguchi H, Mori A, et al. Hexylthiophene-functionalized carbazole dyes for efficient molecular photovoltaics: tuning of solar-cell performance by structural modification. Chem Mater 2008;20:3993–4003.
[24] Lei B-X, Fang W-J, Hou Y-F, Liao J-Y, Kuang D-B, Su C-Y. All-solid-state electrolytes consisting of ionic liquid and carbon black for efficient dye-sensitized solar cells. J Photochem Photobiol A 2010;216:8–14.
[25] Wu TY, Tsao MH, Chen FL, Su SG, Chang CW, Wang HP, et al. Synthesis and characterization of organic dyes containing various donors and acceptors. Int J Mol Sci 2010;11:329–53.
[26] An B-K, Kwon S-K, Jung S-D, Park SY. Enhanced emission and its switching in fluorescent organic nanoparticles. J Am Chem Soc 2002;124:14410–5.
[27] Jones BA, Facchetti A, Wasielewski MR, Marks TJ. Tuning orbital energetics in arylene diimide semiconductors. Materials design for ambient stability of n-type charge transport. J Am Chem Soc 2007;129:15259–78.
[28] Zhang G, Bai Y, Li R, Shi D, Wenger S, Zakeeruddin SM, et al. Employ a bis-thienothiophene linker to construct an organic chromophore for efficient and stable dye-sensitized solar cells. Energy Environ Sci 2009;2:92–5.
[29] Grätzel M. Photoelectrochemical cells. Nature 2001;414:338–44.
[30] Ito S, Zakeeruddin SM, Humphry-Baker R, Liska P, Charvet R, Comte P, et al. High-efficiency organic-dye-sensitized solar cells controlled by nanocrystalline-TiO_2 electrode thickness. Adv Mater 2006;18:1202–5.
[31] Montanari I, Nelson J, Durrant JR. Iodide electron transfer kinetics in dye-sensitized nanocrystalline TiO_2 films. J Phys Chem B 2002;106:12203–10.
[32] Fabregat-Santiago F, Bisquert J, Garcia-Belmonte G, Boschloo G, Hagfeldt A. Influence of electrolyte in transport and recombination in dye-sensitized solar cells studied by impedance spectroscopy. Sol Energy Mater Sol Cells 2005;87:117–31.
[33] Liao J-Y, Lei B-X, Chen H-Y, Kuang D-B, Su C-Y. Oriented hierarchical single crystalline anatase TiO_2 nanowire arrays on Ti-foil substrate for efficient flexible dye-sensitized solar cells. Energy Environ Sci 2012;5:5750–7.